UDC 546.26-162.001.1

Ch. He, L. Z. Sun, J. Zhong (Xiangtan, China)

Prediction of superhard carbon allotropes from the segment combination method

Many superhard allotropes of carbon have been proposed in recent years for the purpose of explaining the superhard carbon phases observed in the processes of cold compressing graphite and carbon nanotubes. In this paper, we have reviewed recent advances in searching for superhard phases of carbon from a segment combination view and found that they can be divided into two groups: (i) combinations of segments from cubic diamond and hexagonal diamond with 5-6-7 carbon rings and (ii) combinations of segments from hexagonal diamond and mutated hexagonal diamond with 4-6-8 carbon rings. Finally, an additional example of extending these allotropes of carbon to their corresponding boron nitride counterparts has been discussed.

Keywords*: superhard material, carbon allotrope, cold compressing graphite, crystal structure prediction, first-principles method.*

INTRODUCTION

Superhard materials are mainly distributed in covalent compounds formed by light elements (boron (B), carbon (C), nitrogen (N), and oxygen (O)) since these elements have ability to form short and strong three-dimensional (3D) covalent bonds to enhance the hardness of the compounds. Among these elements, carbon is considered as the most active one due to its broad *sp*, sp^2, and sp^3 hybridizing ability to bond to itself and to other elements. Although there are many theoretical predictions and experimental discoveries of superhard compounds, such as cBN [1], wBN [2], BC_5 [3, 4], C_3N_4 [5–20], BC_2N [21–30], BCN diamonds [31, 32], and other covalent compounds [12, 18, 20], the hardest material discovered until now is believed to be the pure 3D covalent carbon phase, cubic diamond (C-diamond). In nature, element C mainly exists in its ground state of very soft graphite. Superhard C-diamond, hexagonal diamond (H-diamond), and other diamond allotropes, such as the 4H [33], 6H [33], 8H [34], 9R [34], 12R [35], 15R [34], and 21R [34] carbon allotropes, are metastable states, which can be formed only under proper conditions. The fascinating structures, wide applications and rarity of C-diamond and H-diamond have made them important objects in materials science. Many efforts have been devoted to find proper methods to synthesize C-diamond and H-diamond.

Static compression of graphite is an interesting approach to obtain C-diamond and H-diamond [36–43]. It usually results in H-diamond at high temperatures from 1200 to 1700 K [37, 40–42] and C-diamond at higher temperatures [36, 38–40, 42]. However, in the process of cold compressing graphite, because there is not enough energy to conquer energy barriers between graphite and C-diamond or H-diamond, an unknown superhard phase may be produced [36, 43–46] along with the structural phase transition. This novel superhard phase of carbon has led to many theoretical studies and several structures have been proposed for the purpose of

fitting the experimental data, such as the sp^2–sp^3 graphite–diamond structures [47], monoclinic M-carbon [48] (this carbon allotrope was predicated in 2006 [49] and later identified as a candidate [48] for the experimentally observed superhard graphite [45]), body-centered tetragonal C_4 (bct-C_4) [50] (this allotrope was predicated in 1997 [51], 2004 [52, 53], and 2005 [54] and later identified as a candidate [50] for the experimentally observed superhard graphite [45]), orthorhombic W-carbon [55], and Z-carbon [56–58] (Z-carbon is also named as oC16II [58], Cco-C8 [56], and Z4-A_2B_2 [59]). These theoretical predictions have triggered off many works on searching for low energy superhard carbon allotropes [59–68]. We find that all these previously proposed superhard carbon allotropes are obtained by the designed computer programs, such as the particle–swarm optimization method [58, 62, 69, 70], graph theoretical methods [53], evolutionary algorithm USPEX [49, 61, 64, 66], and the minima hopping method [57, 65, 71] (MHM) for crystal structure prediction [72], or constructed through the schemes reported by Niu [63] and in our latest work [59]. In this paper, we have reviewed these superhard carbon allotropes using segment combination method and found that all of them can be included in two groups: (i) combinations of segments from C-diamond and H-diamond with 5-6-7 carbon rings, and (ii) combinations of segments from H-diamond and mutated H-diamond with 4-6-8 carbon rings. Finally, an interesting example of extending these allotropes of carbon to their corresponding boron nitride counterparts for searching new superhard phases of boron nitride is discussed.

SEGMENT COMBINATION METHOD

Principle description

We noticed that the previously proposed allotropes of carbon can be divided into two groups: 5-6-7-type (M-carbon [48, 49], W-carbon [55], and other phases containing 5, 6, 7 carbon rings) and 4-6-8-type (bct-C_4 [50–54], Z-carbon [56–58], and other phases containing 4, 6, 8 carbon rings). From the point of view of structure, they all can be considered as the combinations of H-diamond and mutated H-diamond, or combinations of H-diamond and C-diamond. Such segment combinations are very similar to the mutations and hybridizations in genetics. The genetic algorithm (GA) is wildly used in searching for stable clusters such as carbon fullerenes [73] and also an effective method in predicting three-dimensional (3D) superhard carbon phases [49]. From the point of view of genetics, since H-diamond and C-diamond are the most favorable sp^3 carbon allotropes in nature, they could be excellent parents for searching for new carbon allotropes through combinations of their gene segments. For example, by stacking carbon layers selected from C-diamond along the [111] direction or H-diamond segments along the [001] direction (such carbon layers have the same carbon configurations as that of chair graphane and we call them H-diamond segments according to the fact that their simple AA stacking can be considered as distorted H-diamond. As mentioned below, the C-diamond segments are defined as carbon layers with same carbon configuration of stirrup graphane), many diamond allotropes were proposed and investigated, such as 4H [33], 6H [33], 8H [34], 9R [34], 12R [35], 15R [34], and 21R [34]. Here, we notice that M-carbon and W-carbon contain carbon layers different to H-diamond segment. Such carbon layers, with the same carbon configuration of stirrup graphane, can be found in C-diamond in the [110] direction but can't be found in H-diamond in any directions, so called as C-diamond segments. Different form previously proposed diamond allotropes containing only

H-diamond segments, M-carbon and W-carbon can be regarded as the combinations of distorted H-diamond segments and distorted C-diamond segments. As indicated in Fig. 1, both M-carbon and W-carbon are layered structures with alternant C-diamond and H-diamond segments. M-carbon and W-carbon are constructed from hybridizing H-diamond segments and C-diamond segments along the [001] direction and [110] direction, respectively, creating interfaces containing 5-7 rings. Deleting all the H-diamond or C-diamond layers in both M-carbon and W-carbon with further lattice compressing, a distorted C-diamond or H-diamond structure (as shown in Fig. 1, *c* and *d*) can be obtained.

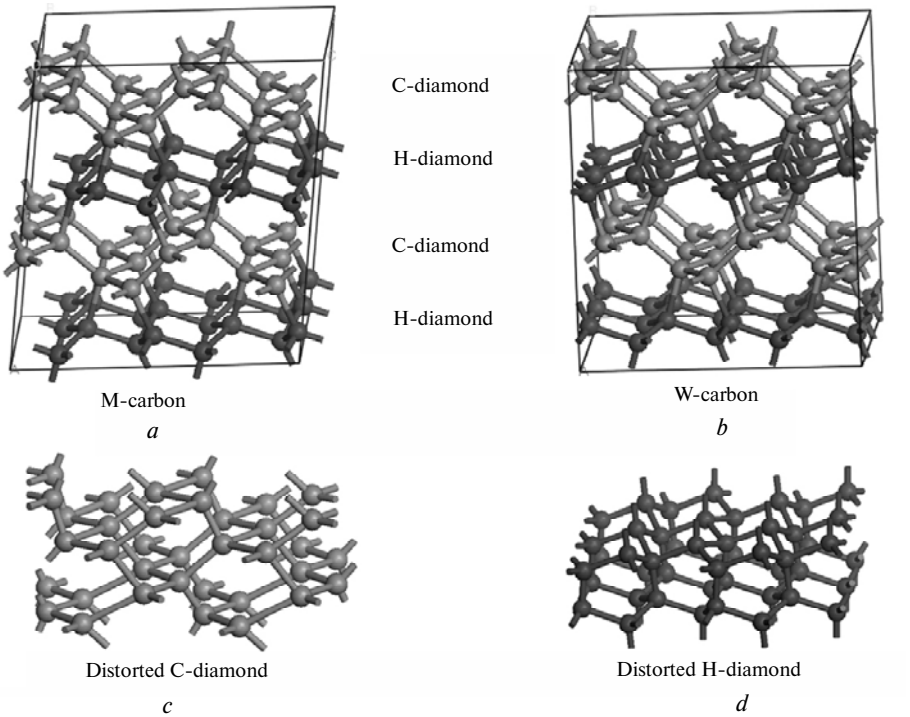

Fig. 1. Crystal structure of M-carbon (*a*) and W-carbon (*b*) with layers of C-diamond and H-diamond. (*c*) and (*d*) indicate the distorted C-diamond and H-diamond, respectively, separated from M-carbon or W-carbon.

For the 4-6-8 type bct-C_4 and Z-carbon shown in Fig. 2, *a* and *b*, we can see that their structural views from the [010] directions are identical to that of graphite from the [001] direction. From the views of their [001] directions, we find that both of them can be regarded as combinations of H-diamond and mutated H-diamonds. In the mutated H-diamond area, there exist some periodic mutated segments translated along the [001] direction with a half-periodicity (c/2) displacement, creating a series of 4 and 8 carbon rings at the interface between the perfect and mutated segments of H-diamond. In summary, we find that from combinations of segments from C-diamond and H-diamond in different manners, almost all previously proposed carbon structures can be obtained. Such structural construction processes are compatible with the essence of GA. In our latest works [59, 67], six superhard carbon allotropes with 5-6-7 (Z-ACA, Z-CACB, H-carbon and S-carbon) and 4-6-8 (Z4-A_3B_1 and A4-A_2B_2) carbon rings were proposed based on this simple segment combination method. Our calculations on their structures, energies, mechanical and electronic properties reveal that all of them are

superhard insulators with direct or indirect band gaps, which are expected to be potential products of cold compressing graphite.

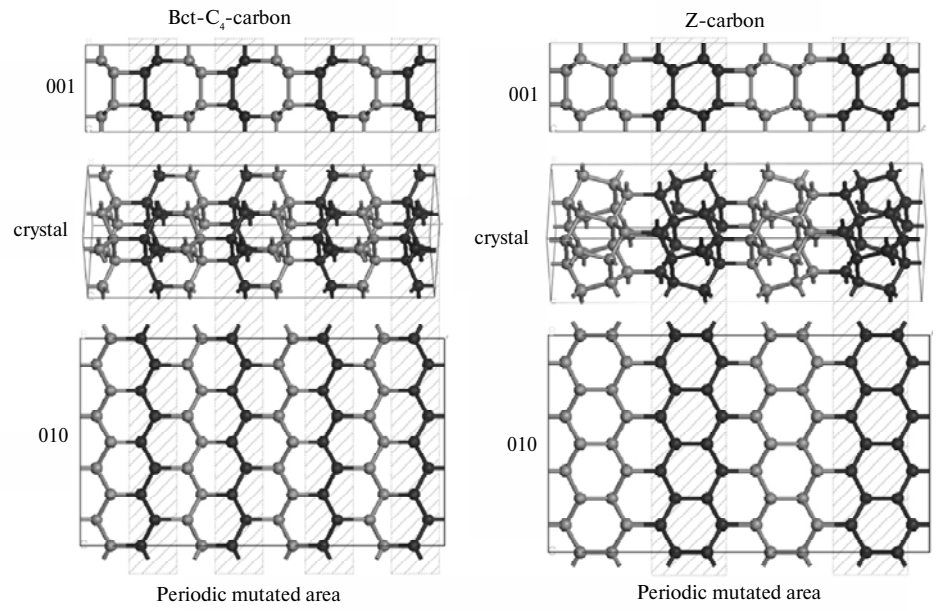

Fig. 2. Views from [001] direction (top), full crystal structure (center) and [010] direction (bottom) of bct-C_4 (*a*) and Z-carbon (*b*). Both structures can be regarded as combinations of segments from H-diamond and mutated H-diamond as indicated in figures.

RESULTS AND DISCUSSION

With the segment combination method enormous superhard carbon allotropes can be constructed. In our investigations [59, 67], we only consider examples with relatively small primitive cells containing no more than 16 carbon atoms. In Fig. 3, *a* we show the situations of hybridizing H-diamond and C-diamond in the zigzag direction with 5-7 carbon rings at the C/A or C/B interface. The systems constructed by hybridizing H-diamond and C-diamond in the armchair direction are energy unstable because the interfacial carbon atoms deflect from the stable four bonds configuration. The four low energy allotropes named as Z-CACB [59], Z-ACA [59], S-carbon [67] (S-carbon also named as C-carbon by D. Li et al. [61]), and H-carbon [67] (H-carbon also named as O-carbon [60] and R-carbon [63] by J. T. Wang et al. and H. Y. Niu et al., respectively) containing 12, 16, 12 and 16 atoms in their primitive cells, respectively, are shown in Fig. 3, *a*. Here, A, B and C denote the segments of the H-diamond, mutated H-diamond, and C-diamond, respectively [59]. In Fig. 3, *b*, we show the 110 view and 001 view of an H-diamond supercell. In the 001 view, the chosen crystal cells for H-diamond, bct-C_4 and Z-carbon are indicated. Especially, the area in the chosen crystal cells of bct-C_4 and Z-carbon indicate the mutated H-diamond segments, which are translated along the [001] direction with a displacement of half-periodicity. One can construct many combinations of H-diamond and mutated H-diamond through introducing periodic mutated H-diamond segments in a properly chosen supercell of H-diamond, such as the previously proposed bct-C_4 and Z-carbon as shown in Fig. 2, *a* and *b*, respectively. We discuss two new of them (Z4-A_3B_1 (this also named as

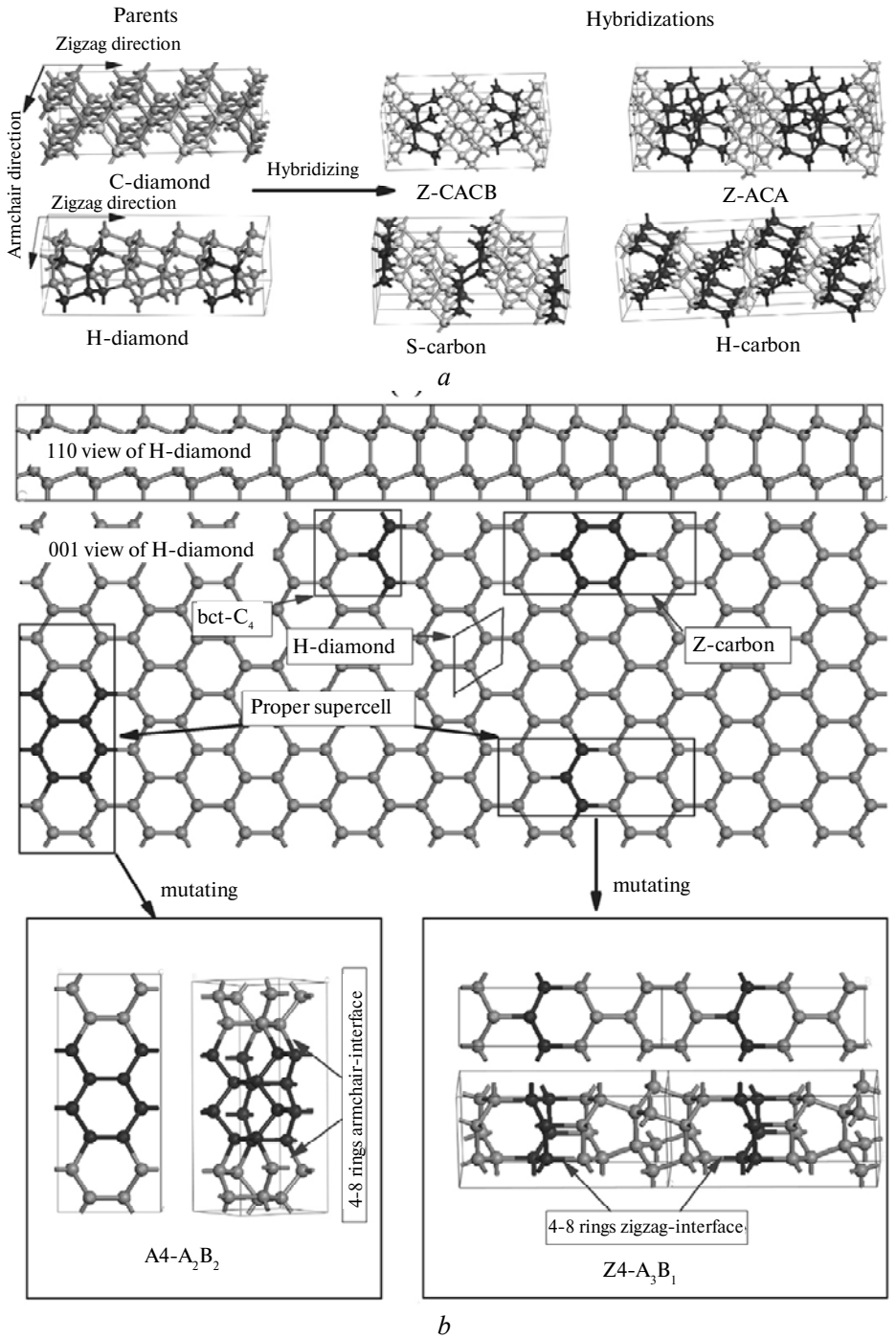

Fig. 3. Hybridizing C-diamond and H-diamond for superhard carbon phases Z-CACB, Z-ACA, S-carbon, and H-carbon (*a*) and mutating H-diamond for superhard carbon phases A4-A_2B_2, and Z4-A_3B_1 (*b*).

P-carbon by H. Y. Niu [63]) and A4-A_2B_2 as shown in Fig. 3, *b*) with relatively small primitive cells and holding remarkable stabilities comparable to bct-C_4. Here Z and A denote that the systems hold 4-8 carbon rings zigzag–interface and armchair–interface, respectively. A and B in Zn-type (An-type) systems denote the

zigzag–segments (armchair–segments) and mutated zigzag–segments (mutated armchair–segments) of H-diamond. Corresponding subscript number denotes the size of the segments. Under this simple nomenclature, Z-carbon composed of two A segments derived from H-diamond and two B segments derived from mutated H-diamond is named as Z4-A_2B_2. At its AA-BB interface, a series of 4-8 carbon rings zigzag–interface occurs. Bct-C_4 with a series of 4-8 carbon rings zigzag–interfaces is named as Z2-A_1B_1 (Z4-$A_1B_1A_1B_1$) according to the fact that there are one A segment and one B segment in its crystal cell. As shown in Fig. 3, *b*, Z4-A_3B_1 is composed by a triple A segment derived from H-diamond and one B segment derived from mutated H-diamond. The primitive cell of A4-A_2B_2 contains 16 carbon atoms and its crystal cell contains one double A segment and one double B segment of H-diamond, forming a series of 4-8 rings armchair-interfaces as shown in Fig. 3, *b*. The systems of A2-A_1B_1 and A4-A 1B1 AiBi are energy less stable than bct-C_4. Z3-systems are restricted according to the topological requirement and the systems of A3-, A4-A_3B_1, Zn- and An- with *n* larger than 4 containing more than 16 atoms in their primitive cells are not considered in our works.

Structures

The fundamental structural information on C-diamond, H-diamond, M-carbon, W-carbon, bct-C_4, Z-carbon, Z-CACB, Z-ACA, S-carbon, H-carbon, A4-A_2B_2, and Z4-A_3B_1 is summarized in Table 1. One can construct these superhard carbon allotropes according to their structural information on space groups, lattice constants, and inequivalent atomic positions summarized in Table 1. For example, S-carbon belongs to the *Cmcm* space group and its equilibrium lattice constants are a = 2.523 Å, b = 11.385 Å and c = 4.899 Å. There are four inequivalent atomic in S-carbon locate at positions of (0.500, 0.778, 0.250), (0.500, 0.442, 0.078), (0.500, 0.132, 0.518), and (0.000, 0.300, 0.750). Among these new allotropes, Z-ACA, Z-CACB, H-carbon, and S-carbon belong to 5-6-7-type similar to M-carbon and W-carbon containing 5-, 6-, and 7-carbon rings. Z4-A_3B_1 and A4-A_2B_2 belonging to 4-6-8-type can be regarded as combinations of H-diamond segments, which are similar to bct-C_4 and Z-carbon.

Structurally, all these new carbon allotropes can be considered as potential products in the process of cold compressing graphite.

Stability

The relative stability of these superhard carbon allotropes is evaluated by comparing their enthalpy per atom at a wide range of pressure from 0 to 40 GPa. From the cohesive energies per atom listed in Table 2 and the relative enthalpy–pressure curves shown in Fig. 4, we can see that Z-CACB, Z-ACA, S-carbon, H-carbon, A4-A_2B_2, and Z4-A_3B_1 are more favorable than bct-C_4. At zero pressure, the cohesive energy of Z-ACA is about 30 meV lower than bct-C_4 and only 5 meV higher than that of M-carbon. When the pressure is larger than 10 GPa, it becomes more favorable than M-carbon and comparable to W-carbon when pressure is above 35 GPa. Z-CACB, S-carbon, H-carbon, A4-A_2B_2, and Z4-A_3B_1 are more favorable than both M-carbon and W-carbon at the pressure range of 0–40 GPa. Especially, S-carbon (–7.593 eV) among them holds energy only 100 meV per atom larger than that of C-diamond (–7.693 eV), becoming the most stable one with about 25 meV per atom lower than the second stable Z4-A_3B_1 (–7.568). In comparison with graphite, all these superhard allotropes are metastable phases at zero pressure. With the increase of pressure, the most stable S-carbon becomes

more stable than graphite when pressure is above 5.93 GPa. The following three allotropes with almost the same transition pressure, namely, Z4-A_3B_1, A4-A_2B_2, and Z-carbon become more favorable than graphite when the pressure is larger than 9.16 GPa. The transition pressures for M-carbon, W-carbon, Z-ACA, and H-carbon are very close to each other (located at the pressure range from 12.1 to 13.3 GPa). Z-CACB is always more favorable than bct-C_4, M-carbon, W-carbon, Z-ACA, and H-carbon in a wide pressure range from 0 to 40 GPa and it becomes more stable than graphite, when the pressure is larger than 10 GPa. When the pressure is larger than 18.29 GPa, the least stable bct-C_4 among these allotropes becomes more favorable than graphite. The results indicate that all of these superhard allotropes may be transformed from graphite with high enough external pressure. To further confirm the dynamic stability of Z-CACB, Z-ACA, S-carbon, H-carbon, A4-A_2B_2, and Z4-A_3B_1, their phonon band structures and phonon density of states are calculated. According to our calculations, there is no imaginary frequency in the phonon band structures of all these new carbon allotropes up to 40 GPa, confirming that these allotropes are dynamically stable phases of carbon.

Table 1. GGA calculated structural information for C-diamond, H-diamond, M-carbon, W-carbon, bct-C_4, Z-carbon, Z-CACB, Z-ACA, S-carbon, H-carbon, A4-A_2B_2, and Z4-A_3B_1 at 0 GPa

System	Space group and cell	Inequivalent atomic position	Rings type
C-diamond	*Fd*-3*m* (No. 227)	(0.250, 0.250, 0.250)	6
Z-CACB	*Imma* (No. 74)	(0.500, 0.750, 0.542)	5-6-7
	a = 4.876 Å, b = 2.529 Å, c = 11.535 Å	(0.237, 0.750, 0.618)	
		(0.177, 0.250, 0.691)	
		(0.500, 0.750, 0.965)	
Z-ACA	*Pmmn* (No. 59)	(0.000, 0.500, –0.069)	5-6-7
	a = 4.760 Å, b = 2.521 Å, c = 7.930 Å	(–0.500, 0.500, –0.043)	
		(–0.265, 0.500, –0.171)	
		(–0.326, 1.000, –0.276)	
		(–0.196, 1.000, –0.453)	
S-carbon	*Cmcm* (No. 63)	(0.500, 0.778, 0.250)	5-6-7
	a = 2.523 Å, b = 11.385 Å, c = 4.899 Å	(0.500, 0.442, 0.078)	
		(0.500, 0.132, 0.518)	
		(0.000, 0.300, 0.750)	
H-carbon	*Pbam* (No. 55)	(0.046, 0.361, 0.500)	5-6-7
	a = 7.874 Å, b = 4.807 Å, c = 2.524 Å	(0.157, 0.309, 0.000)	
		(0.327, 0.462, 0.000)	
		(0.430, 0.393, 0.500)	
A4-A_2B_2	*Cmca* (No. 64)	(0.317, 0.067, 0.088)	4-6-8
	a = 4.257 Å, b = 10.114 Å, c = 4.363 Å	(0.314, 0.188, 0.584)	
Z4-A_3B_1	*Pmmn* (No. 59)	(0.041, 0.312, 0.500)	4-6-8
	a = 8.762 Å, b = 4.263 Å, c = 2.514 Å	(0.208, 0.185, 0.500)	
		(0.285, 0.316, 1.000)	
		(0.464, 0.318, 1.000)	

Table 2. The mass density (D, g/cm^3), band gap (E_g, eV), cohesive energy (E_{coh}, eV), bulk modulus (B_0, GPa), and Vickers hardness (H_V, GPa) for diamond, M-carbon, W-carbon, bct-C_4, Z-carbon, Z-CACB, Z-ACA, S-carbon, H-carbon, A4-A_2B_2, and Z4-A_3B_1

Systems	D	E_g	E_{coh}	B_0	H_V
Diamond	3.496	4.635(I)	–7.693	473.72	88.32
M-carbon	3.336	3.493(I)	–7.531	404.58	79.24
W-carbon	3.346	4.281(I)	–7.539	400.29	79.08
Bct-C_4	3.309	2.491(I)	–7.497	401.91	67.59
Z-carbon	3.399	3.273(I)	–7.564	415.83	81.09
Z-CACB	3.365	4.196(D)	–7.556	405.41	82.01
Z-ACA	3.353	2.261(D)	–7.526	375.97	78.74
S-carbon	3.401	4.342(D)	–7.593	416.23	79.55
H-carbon	3.341	4.459(I)	–7.554	400.94	76.92
A4-A_2B_2	3.397	3.271(I)	–7.565	413.62	83.18
Z4-A_3B_1	3.398	3.105(I)	–7.568	415.49	80.54

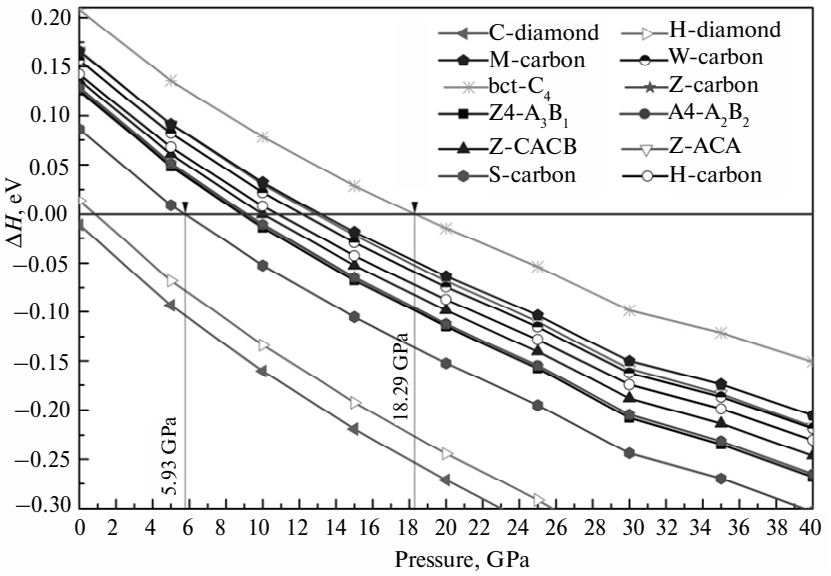

Fig. 4. The enthalpy per atom for C-diamond, H-diamond, M-carbon, W-carbon, bct-C_4, Z-carbon, Z-CACB, Z-ACA, S-carbon, H-carbon, A4-A_2B_2, and Z4-A_3B_1 as a function of pressure relative to graphite.

Mechanical and electronic properties

The mass density, energy band gap, bulk modulus, and Vickers hardness of diamond, M-carbon, W-carbon, Z-carbon, bct-C_4, Z-CACB, Z-ACA, S-carbon, H-carbon, A4-A_2B_2, and Z4-A_3B_1 are summarized in Table 2. The results indicate that all above carbon allotropes are superhard intermediate phases between graphite and diamond due to their considerable bulk modulus and hardness. In our studies [59, 67], the values of the bulk modulus (B_0) were obtained by fitting the total energy as a function of volume to the third-order Birch-Murnaghan equation of state. Also many theoretical models have been proposed to do further hardness evaluation [74–79]. Here, our results of hardness

are evaluated according to the recently proposed one [74], which correlates the Vickers hardness (H_V) to the bulk modulus (B_0) and shear modulus (G) through the formula: $H_V = 2(G^3/B^2)^{0\,585} - 3$. From Table 2, we can see that bct-C_4 holds the least stability, mass density, bulk modulus, and hardness in comparison with other allotropes. The Z-carbon, S-carbon, A4-A_2B_2, and Z4-A_3B_1 hold almost the same stability, band gap, mass density, bulk modulus, and hardness. The values of bulk modulus (Vickers hardness) are 415.83 GPa (81.09 GPa), 416.23 GPa (79.55 GPa), 413.62 GPa (83.18 GPa), and 415.49 GPa (80.54 GPa) for Z-carbon, S-carbon, A4-A_2B_2, and Z4-A_3B_1, respectively. M-carbon, W-carbon, Z-CACB, Z-ACA, and H-carbon hold similar stability, density, bulk modulus, and Vickers hardness. Their calculated values of Vickers hardness are 79.24 GPa, 79.08 GPa, 82.01 GPa, 78.74 GPa, and 76.92 GPa, respectively. The results indicate that all these potential carbon allotropes are superhard materials comparable to diamond (88.32 GPa).

We also studied the electronic properties of diamond, M-carbon, W-carbon, Z-carbon, bct-C_4, Z-CACB, Z-ACA, S-carbon, H-carbon, A4-A_2B_2, and Z4-A_3B_1 [59, 67]. The band structures of Z-CACB, Z-ACA, S-carbon, H-carbon, A4-A_2B_2, and Z4-A_3B_1 are shown in Figs. 5*a*–5*f*, respectively. The results indicate that all these superhard carbon allotropes have indirect wide band gaps except for Z-CACB, Z-CAC, and S-carbon. The band gaps are 4.635, 3.493, 4.281, 2.491, and 3.273 eV for C-diamond, M-carbon, W-carbon, bct-C_4, and Z-carbon, respectively. The band gaps of Z-CACB, Z-ACA, S-carbon, H-carbon, A4-A_2B_2, and Z4-A_3B_1 are 4.196, 2.261, 4.342, 4.459 eV, 3.271, and 3.105 eV, respectively. From the results summarized in Table 2 and shown in Fig. 4, we can see that except for bct-C_4 and Z-CAC with relatively narrow band gaps, all other superhard carbon allotropes are transparent insulators with wide band gaps.

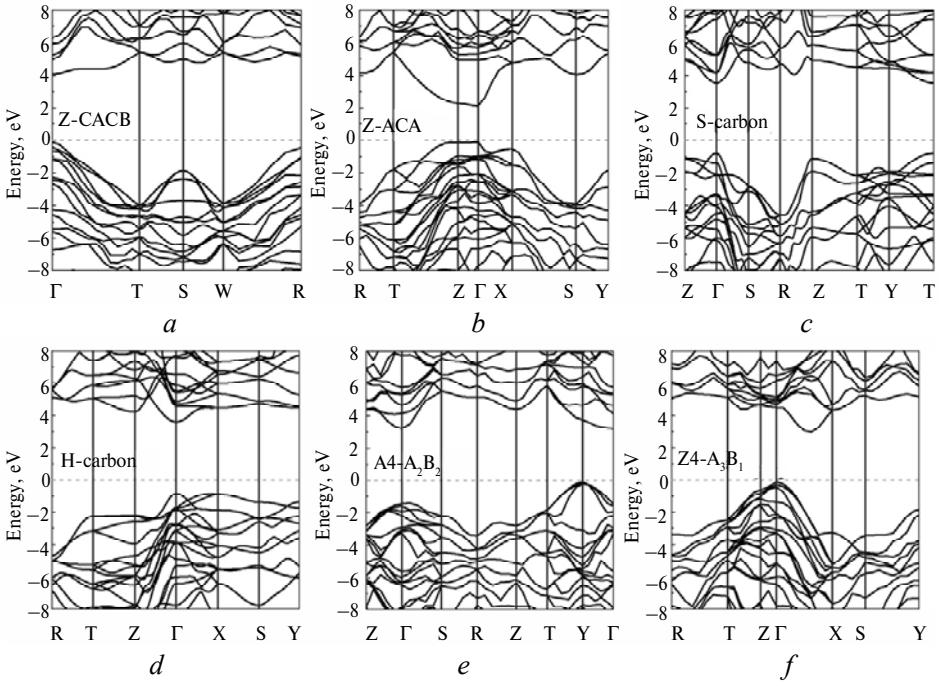

Fig. 5. The calculated band structures (at zero pressure) for Z-CACB (*a*), Z-ACA (*b*), S-carbon (*c*), H-carbon (*d*), A4-A_2B_2 (*e*), and Z4-A_3B_1 (*f*).

ADDITIONAL DISCUSSIONS

Six low energy superhard carbons had been successfully predicted by simple segment combination method. We should point out that such a segment combination method is a special method in searching for low energy superhard carbon allotropes. It is not a universal method of crystal prediction like the particle–swarm optimization method [58, 62, 69, 70], graph theoretical methods [53], evolutionary algorithm USPEX [49, 61, 64, 66], and the minima hopping method [57, 65, 71] (MHM) for crystal structure prediction [72], which can predict elements crystals from just the chemical composition.

All the previously proposed carbon phases can not singly fit the experimental results satisfactorily. In view of the cohesive energy, dynamical stability, electronic structure, bulk modulus, the lowest phase transition pressure point and transition pathway avoiding the slippage from *AB*- to *AA*-stacking graphite (which may cost additional energy to conquer the barrier between *AB*-stacking graphite and *AA*-stacking graphite), H-carbon, and S-carbon are expected to be easily formed in cold compressing graphite. The simulated X-ray diffraction (XRD) patterns for graphite, Z-carbon, H-carbon, and S-carbon at pressure of 23.9 GPa are shown in Fig. 6 to compare with the experimental data provided by Mao et al. [45]. The experimental data under high pressure can be explained by H-carbon and S-carbon to some extent. The main XRD peaks located in the region between 8.5–11° and 15–17° for H-carbon and S-carbon agree well with the experimental observation. However, as indicated by Amsler et al. [57], the sole comparison between experimental and theoretical XRD cannot directly clarify the new carbon phase. Further evidences such as Raman spectra and transition barrier are needed.

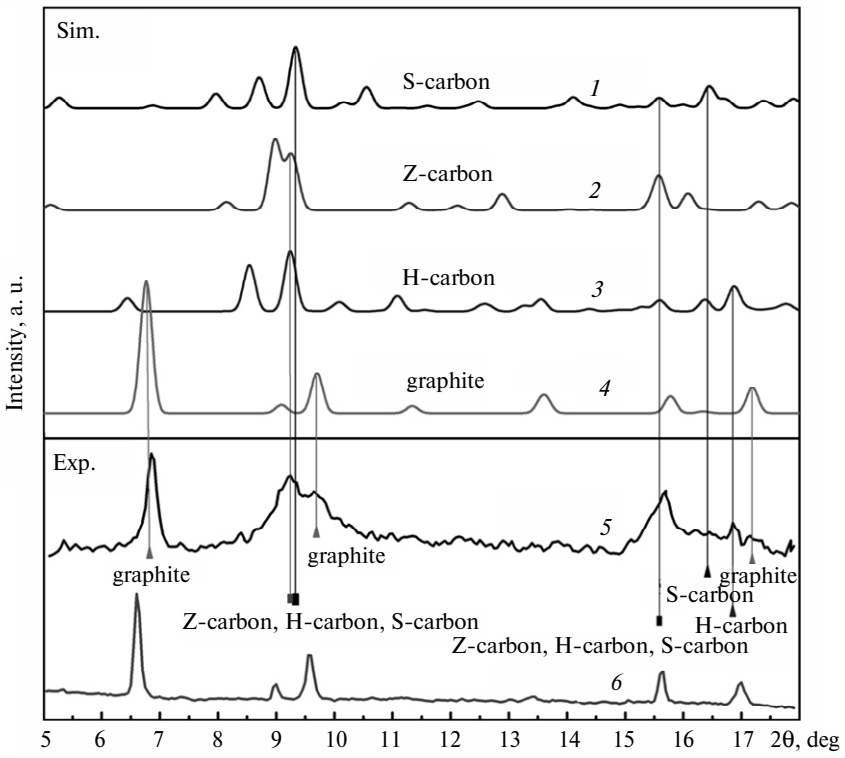

Fig. 6. Simulated XRD data for S-carbon, Z-carbon, H-carbon, and graphite at corresponding pressure as well as the experimental XRD data at 23.9 (*1–5*) and 13.7 (*6*) GPa for the superhard intermediate state derived from cold compressing graphite [45].

To date many carbon allotropes have been proposed as the potential products of cold compressing graphite. In fact, interests have been expressed not only in the search for low energy structures but also in corresponding transformation pathways from graphite [35, 55, 60, 80–83]. The transformation pathways are more significant for further evaluating the probabilities to form these proposed superhard carbon allotropes by cold compressing graphite. The particular nucleation history [82] is very important during the phase transition process depending on the starting graphitic structure and the final phases. Formation of different phases needs to conquer different barriers. Some previous investigations of transformation pathways from graphite to metastable M-carbon, bct-C_4, W-carbon, and O-carbon (H-carbon) are based on the nudged elastic band method [35, 55, 60, 81]. These investigations provide inconsistent results of the transition barriers sequence. As discussed by Boulfelfel et al. recently [83], at zero pressure Zhou et al. [81] reported that the barrier to bct-C_4 is lower than those to M-carbon and C-diamond, but Wang et al. reported a barriers sequence of W-carbon < M-carbon < C-diamond < bct-C_4. Using state-of-the-art molecular dynamics transition path sampling simulations, Boulfelfel et al. investigated the kinetic pathways of the pressure-induced transformation of graphite to M-carbon, W-carbon, and bct-C_4. Their results demonstrate that the characteristic nucleation pattern leads to M-carbon as a final product rather than to W-carbon and bct-C_4. A recent experimental work also suggests that cold compressing graphite results in M-carbon [84] rather than in bct-C_4, W-carbon, and Z-carbon. Although these experimental and theoretical works provide us timing and important evidence to believe that the superhard phase obtained in cold compressing graphite is M-carbon, it is interesting to investigate the transition pathways from graphite to the other proposed superhard carbons.

SUPERHARD BORON NITRIDE PHASES

As mentioned previously, many theoretical efforts have been made in search low energy superhard carbon allotropes. In comparison with those efforts made in carbon phases, relatively less theoretical attention is given to searching for superhard BN phases. In fact, boron nitride has many polymorphs, such as hexagonal BN (hBN) [85], zinc blende BN (cBN) [1], wurtzite BN (wBN) [2], amorphous BN [86], BN nanotubes [87], and BN fullerenes [88], which can be considered as counterparts of graphite, C-diamond, H-diamond, amorphous carbon, carbon nanotubes, and fullerenes. Superhard wBN and cBN have received intense attention owing to their excellent optical, electrical, and mechanical properties. The phase transitions from soft hBN to hard cBN and wBN have been interesting issues for decades and attracted many theoretical [89–92] and experimental efforts [86, 93, 94]. However, the mechanisms of such transitions are still ambiguous. For example, cold compressing hBN always results in the metastable wBN instead of the stable cBN [93]. To understand this, the transformation mechanism between hBN and wBN phases have been wildly investigated [95–98]. Wen et al. [97] suggested that there might be some intermediate states between hBN and wBN, and proposed a new BN phase (bct-BN) [97] with considerable stability and excellent mechanical properties (this novel bct-BN phase was also investigated by other groups [98, 99]). Similar to the cold compression of graphite, cold compressing hBN may results in some unknown intermediate states. More theoretical efforts are needed in search for the potential intermediate BN phases in cold compressing hBN.

There are many similar characteristics between carbon and BN systems, implying that all the proposed carbon allotropes might be excellent templates for finding superhard BN phases. We notice that bct-BN [97–99] is a counterpart system of bct-C_4 carbon. It is worthy to extend other superhard carbon phases to their corresponding BN counterpart systems to design new superhard BN phases. In fact, the transforming path from hBN to bct-BN has been studied by Wen et al. [97] and their results show that M-BN is energy unstable due to the existence of the boron–boron (B–B) and nitrogen–nitrogen (N–N) bonds. We believe that BN phases with the structures of M-carbon, W-carbon, Z-CACB, Z-ACA, S-carbon, and H-carbon are expected to be energy unstable due to the existence of five-seven patterns in such structures. Similar to bct-C_4, the structures of Z-carbon, A4-A_2B_2, and Z4-A_3Bi are excellent templates for new BN phases because their structures contain only even carbon rings (four-eight carbon rings). In our recent work [100], we have investigated the structure, stability, mechanical and electronic properties of the potential BN phases with the structures of bct-C_4 and Z-carbon, both of which can be regarded as the mutations of wBN, as their corresponding counterpart systems bct-C_4 and Z-carbon are the mutations of H-diamond [59].

Figures 7, *a* and *b* show the crystal views of bct-BN and Z-BN from the [010] (top) and [001] (bottom) directions. The detailed structure information of bct-BN and Z-BN can be found in our work [100]. From Fig. 7, we can see that the apparent difference between these two new BN phases is the absence of hexagon pattern for bct-BN viewed from their [001] direction. The structures of both bct-BN and Z-BN are constructed with the four–eight patterns but without the five-seven patterns as those in M-carbon, W-carbon, Z-CACB, Z-ACA, S-carbon, and H-carbon. Moreover, from the structural point of view, both bct-BN and Z-BN can be regarded as mutations of wBN and can be considered as potential products in the process of cold compressing the AB-stacked [101] hBN. Figure 7, *c* shows the enthalpy per BN pair for cBN, wBN, bct-BN as well as Z-BN as functions of pressure relative to AB-stacked hBN. The results indicate that when the pressure is larger than 3.3 GPa (5.5 GPa), Z-BN (bct-BN) is more stable than hBN. The transition pressure point of Z-BN (bct-BN) from hBN under pressure is 3.3 GPa (5.5 GPa). Z-BN is always more favorable than bct-BN in the pressure range from 0 to 30 GPa, which is similar to the case where Z-carbon is always more favorable than bct-C_4 carbon. In our work, the dynamic stabilities of bct-BN and Z-BN were confirmed by their phonon band structures and phonon density of states [100].

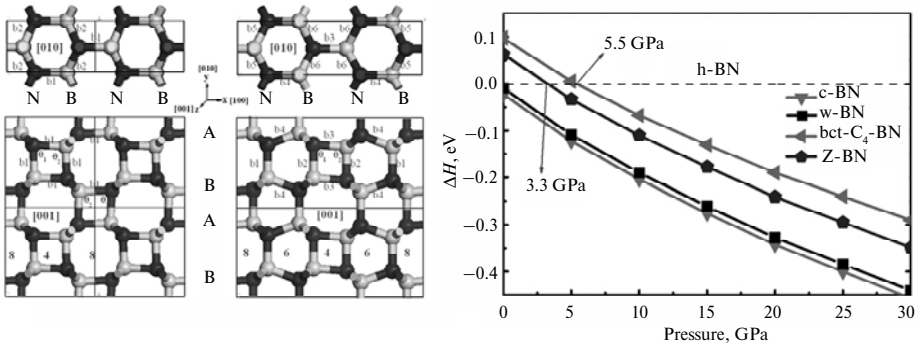

a *b* *c*

Fig. 7. Views from [010] direction (top) and [001] direction (bottom) of bct-BN: θ_1 = 85.84, θ_2 = 94.15, b1 = 1.601, b2 = 1.541 (*a*); Z-BN: θ_1 = 85.58, θ_2 = 94.41, b1 = b2 = 1.595, b3 = 1.578, b4 = 1.594, b5 = 1.554, b6 = 1.551 (*b*) and the enthalpy per BN for cBN, wBN, bct-BN, and Z-BN as a function of pressure relative to hBN (*c*).

The values of bulk modulus of bct-BN (348.35 GPa) and Z-BN (359.61 GPa) are comparable to those for cBN (376.19 GPa) and wBN (375.24 GPa). The values of Vickers hardness for bct-BN, Z-BN, wBN, and cBN are 46.86, 55.88, 63.82, and 62.82 GPa, respectively. These results indicate that Z-BN is a superhard material comparable to cBN. The electronic structures of Z-BN and bct-BN indicate that both systems are indirect-wide-band-gap insulators. The band gap of bct-BN is 4.83 eV, which is in good agreement with previous first-principles calculation [97]. The band gap of Z-BN is 5.27 eV, which is larger than those of cBN, wBN, and bct-BN. Both Z-BN and bct-BN are transparent superhard materials.

CONCLUSIONS

We have reviewed recent advances in searching for superhard carbon phases. From the point of view of segment combinations, we have found that all the recently proposed superhard allotropes of carbon can be divided into two groups: (i) combinations of segments from cubic diamond and hexagonal diamond with 5-6-7 carbon rings, and (ii) combinations of segments from hexagonal diamond and mutated hexagonal diamond with 4-6-8 carbon rings. H-diamond and C-diamond are the most favorable sp^3 carbon allotropes in nature that can be considered as excellent parents for searching for more new carbon allotropes through hybridizing their segments. We emphasize that future efforts should not only be devoted to search for low energy carbon allotropes. Systematical investigations on the transformation pathways from graphite to superhard phases are also significant. Finally, an interesting example of extending these allotropes of carbon to their corresponding boron nitride counterparts to search for new superhard BN phases has been discussed.

ACKNOWLEDGMENTS

This work is supported by the National Natural Science Foundation of China (Grant Nos. 11074211, 511172191, 10874143, and 10974166), the National Basic Research Program of China (2012CB921303), the Cultivation Fund of the Key Scientific and Technical Innovation Project, the Program for New Century Excellent Talents in University (Grant No. NCET-10-0169), and the Scientific Research Fund of Hunan Provincial Education Department (Grant Nos. 10K065, 10A118, 09K033).

В останні роки було запропоновано безліч надтвердих алотропів вуглецю для пояснення його надтвердих фаз, які спостерігають в процесах холодного стиснення графіту і вуглецевих нанотрубок. У даній статті розглянуто останні досягнення в пошуках надтвердих фаз вуглецю з погляду методу комбінації структурних сегментів і виявлено, що вони можуть бути розділені на дві групи: 1) сполучення сегментів кубічного алмазу і гексагонального алмазу з 5-6-7-членними кільцями вуглецю і 2) сполучення сегментів гексагонального і мутованого гексагонального алмазу з 4-6-8-членними вуглецевими кільцями. Нарешті, розглядається відповідність алотропів вуглецю можливим структурам нітриду бору.

***Ключові слова**: надтверді матеріал, вуглецевий алотроп, холодне стиснення графіту, прогнозування кристалічної структури, першопринципні методи.*

В последние годы было предложены много сверхтвердых аллотропов углерода для объяснения его сверхтвердых фаз, наблюдаемых в процессах холодного сжатия графита и углеродных нанотрубок. В данной статье рассмотрены последние достижения в поиске сверхтвердых фаз углерода с точки зрения метода комбинации структурных сегментов и обнаружено, что они могут быть разделены на две группы: 1) сочетания сегментов кубического и гексагонального алмаза с 5-6-7-членными кольцами углерода и 2) сочетания сегментов гексагонального и мутированного гексагонального

алмаза с 4-6-8-членными углеродными кольцами. Наконец, рассматривается соответствие этих аллотропов углерода возможным структурам нитрида бора.

***Ключевые слова**: сверхтвердые материалы, углеродные аллотропы, холодное сжатие графита, предсказание кристаллических структур, первопринципные методы.*

1. *Mirkarimi P. B., McCarty K. F., Medlin D. L.* Review of advances in cubic boron nitride film synthesis // Mater. Sci. Eng, R. – 1997. – **21**, N 2. – P. 47–100.
2. *Bundy F. P., Wentorf R. H.* Direct transformation of hexagonal boron nitride to denser forms // J. Chem. Phys. – 1963. – 38, N 5. – P. 1144–1149.
3. *Solozhenko V. L., Kurakevych O. O., Andrault D. et al.* Ultimate metastable solubility of boron in diamond: synthesis of superhard diamond-like BC_5. – Phys. Rev. Lett. – 2009. – **102**, N 1, art. 015506.
4. *Li Q., Wang H., Tian Y. J. et al.* Superhard and superconducting structures of BC_5 // J. Appl. Phys. – 2010. – **108**, N 2, art. 023507.
5. *Liu A. Y., Cohen M. L.* Prediction of new low compressibility solids // Science. – 1989. – **245**, N 4920. – P. 841–842.
6. *Cohen M. L.* Calculation of bulk moduli of diamond and zinc-blende solids // Phys. Rev. B. – 1985. – **32**, N 12. – P. 7988–7991.
7. *Martin-Gil J., Martin-Gil F. J., Sarikaya M. et al.* Evidence of a low compressibility carbon nitride with defect-zinc-blende structure // J. Appl. Phys. – 1997. – **81**, N 6. – P. 2555–2559.
8. *Yu K. M., Cohen M. L., Haller E. E. et al.* Observation of crystalline C_3N_4 // Phys. Revs. B. – 1994. – **49**, N 7. – P. 5034–5037.
9. *John V. B.* Solid-state carbon nitrides // Adv. Mater. – 1997. – **9**, N 11. – P. 877–886.
10. *Matsumoto S., Xie, E.-Q., Izumi F.* On the validity of the formation of crystalline carbon nitrides, C_3N_4 // Diam. Relat. Mater. – 1999. – **8**, N 7. – P. 1175–1182.
11. *Montigaud H., Tanguy B., Demazeau G. et al.* C_3N_4: Dream or reality? Solvothermal synthesis as macroscopic samples of the C_3N_4 graphitic form // J. Mater. Sci. – 2000. – **35**, N 10. – P. 2547–2552
12. *Marton D., Boyd K. J., Al-Bayati A. H. et al*. Carbon nitride deposited using energetic species: a two-phase system // Phys. Rev. Lett. – 1994. – **73**, N 1. – P. 118–121.
13. *Niu C., Lu Y. Z., Lieber C. M*. Experimental realization of the covalent solid carbon nitride // Science. – 1993. – **261**, N 5119. – P. 334–337.
14. *Sjostrom H., Stafstrom S., Boman M., Sundgren J.-E.* Superhard and elastic carbon nitride thin films having fullerene-like microstructure // Phys. Rev. Lett. – 1995. – **75**, N 7. – P. 1336–1339.
15. *Wixom M. R.* Chemical preparation and shock wave compression of carbon nitride precursors // J. Am. Ceram. Soc. – 1990. – **73**, N 7. – P. 1973–1978.
16. *Peng Y. G., Ishigaki T., Horiuchi S.* Cubic C_3N_4 particles prepared in an induction thermal plasma // Appl. Phys. Lett. – 1998. – **73**, N 25. – P. 3671–3673.
17. *Cao C. B., Lv Q., Zhu H. S.* Carbon nitride prepared by solvothermal method // Diam. Relat. Mater. – 2003. – **12**, N 3–7. – P. 1070–1074.
18. *Mo S.-D., Ouyang L., Ching W. Y. et al.* Interesting physical properties of the new spinel phase of Si_3N_4 and C_3N_4 // Phys. Rev. Lett. – 1999. – **83**, N 24. – P. 5046–5049.
19. *Teter D. M., Hemley R. J.* Low-compressibility carbon nitrides // Science. – 1996. – **271**, N 5245. – P. 53–55.
20. *Li Q., Wang H., Ma Y. M.* Predicting new superhard phases // Superhard Mater. – 2010. – **32**, N 3. – P. 192–204.
21. *Sun J., Zhou X. F., Qian G. R*. et al. Chalcopyrite polymorph for superhard BC_2N // Appl. Phys. Lett. – 2006. – **89**, N 15, art. 151911.
22. *Luo X., Guo X., Xu B. et al*. Body-centered superhard BC_2N phases from first principles // Phys. Rev. B. – 2007. – **76**, N 9, art. 094103.
23. *Luo X., Guo X., Liu Z. et al.* First-principles study of wurtzite BC_2N // Ibid. – 2007. – **76**, N 9, art. 92107.
24. *Zhou X. F., Sun J., Fan Y. X. et al.* Most likely phase of superhard BC_2N by *ab initio* calculations // Ibid. – 2007. – **76**, N 10, art. 100101.
25. *Zhou X. F., Sun J., Qian Q. R. et al.* A Tetragonal phase of superhard BC_2N // J. Appl. Phys. – 2009. – **105**, N 9, art. 093521.

26. *Solozhenko V. L., Andrault D., Fiquet G. et al.* Synthesis of superhard cubic BC_2N // Appl. Phys. Lett. – 2001. – **78**, N 10. – P. 1385–1387.
27. *Sun H., Jhi S.-H., Roundy D. et al*. Structural forms of cubic BC_2N // Phys. Rev. B. – 2001. – **64**, N 9, art. 094108.
28. *Zhang Y., Sun H., Chen C. F.* Superhard cubic BC_2N compared to diamond // Phys. Rev. Lett. – 2004. – **93**, N 19, art. 195504.
29. *Chen S. Y., Gong X. G., Wei S.-H*. Superhard pseudocubic BC_2N superlattices // Ibid. – 2007. – **98**, N 1, art. 015502.
30. *Li Q., Wang M., Oganov A. R. et al.* Rhombohedral superhard structure of BC_2N // J. Appl. Phys. – 2009. – **105**, N 5, art. 053514.
31. *Kawaguchi M., Kawashima T., Nakajima T.* Syntheses and structures of new graphite-like materials of composition BCN(H) and BC_3N(H) // Chem. Mater. – 1996. – **8**, N 6. – P. 1197–1201.
32. *Liu X. B., Jia X. P., Zhang Z. F. et al.* Synthesis and characterization of new "BCN" diamond under high pressure and high temperature conditions // Cryst. Growth Des. – 2011. – **11**, N 4. – P. 1006–1014.
33. *Raffy C., Furthmuller J., Bechstedt F.* Properties of hexagonal polytypes of group-iv elements from first-principles calculations // Phys. Rev. B. – 2002. – **66**, N 7, art. 075201.
34. *Wen B., Zhao J. J., Bucknum M. J. et al*. First-principles studies of diamond polytypes // Diamond Relat. Mater. – 2008. – **17**, N 3. – P. 356–364.
35. *Wang J. T., Chen C. F., Kawazoe Y.* Mechanism for direct conversion of graphite to diamond // Phys. Rev. B. – 2011. – **84**, N 1, art. 012102.
36. *Bundy F. P.* Direct Conversion of graphite to diamond in static pressure apparatus // Science. – 1962. – **137**, N 3535. – P. 1057–1058.
37. *Bundy F.* Direct conversion of graphite to diamond in static pressure apparatus // J. Chem. Phys. – 1963. – 38, N 3. – P. 631–643.
38. *Bundy F. P.* Kasper J. S. Hexagonal diamond – a new form of carbon // Ibid. – 1967. – **46**, N 9. – P. 3437–3446.
39. *Irifune T., Kurio A., Sakamoto S. et al.* Ultrahard polycrystalline diamond from graphite // Nature. – 2003. – **421**. – P. 599–600.
40. *Britun V. F., Kurdyumov A. V., Petrusha I. A.* Diffusionless nucleation of lonsdaleite and diamond in hexagonal graphite under static compression // Powder Metall. Met. Ceram. – 2004. – **43**, N 1. – P. 87–93.
41. *Sumiya H., Yusa H., Inoue T. et al.* Conditions and mechanism of formation of nano-polycrystalline diamonds on direct transformation from graphite and non-graphitic carbon at high pressure and temperature // High Pressure Res. – 2006. – **26**, N 2. – P. 63–69.
42. *Ohfuji H., Kuroki K.* Origin of unique microstructures in nano-polycrystalline diamond synthesized by direct conversion of graphite at static high pressure // J. Mineral. Petrol. Sci. – 2009. – **104**, N 5. – P. 307–312.
43. *Yagi T., Utsumi W., Yamakata M. et al.* High-pressure in situ X-ray diffraction study of the phase transformation from graphite to hexagonal diamond at room temperature // Phys. Rev. B. – 1992. – **46**, N 10. – P. 6031–6039.
44. *Hanfland M., Beister H., Syassen K.* Graphite under pressure: equation of state and first-order raman modes // Ibid. – 1989. – **39**, N 17. – P. 12598–12603.
45. *Mao W. L., Mao H. K., Eng P. J. et al.* Bonding changes in compressed superhard graphite // Science. – 2003. – **302**, N 17. – P. 425–427
46. *Miller E. D., Nesting D. C., Badding J. V.* Quenchable transparent phase of carbon // Chem. Mater. – 1997. – **9**, N 1. – P. 18–22.
47. *Ribeiro F. J., Tangney P., Louie S. G., Cohen M. L.* Structural and electronic properties of carbon in hybrid diamond-graphite structures // Phys. Rev. B. – 2005. – **72**, N 21, art. 214109.
48. *Li Q., Ma Y. M., Oganov A. R. et al.* Superhard monoclinic polymorph of carbon // Phys. Rev. Lett. – 2009. – **102**, N 17, art. 175506.
49. *Oganov A. R., Glass C. W.* Crystal structure prediction using ab initio evolutionary techniques: principles and applications // J. Chem. Phys. – 2006. – **124**, N 24, art. 244704.
50. *Umemoto K., Wentzcovitch R. M., Saito S., Miyake T.* Body-centered tetragonal C_4: a viable sp^3 carbon allotrope // Phys. Rev. Lett. – 2010. – **104**, N 12, art. 125504.
51. *Baughman R. H., Liu A. Y., Cui C. Schields P. J.* A Carbon phase that graphitizes at room temperature // Synth. Met. – 1997. – **86**, N 1. – P. 2371–2374.

52. *Domingos H. S.* Carbon allotropes and strong nanotube bundles // J. Phys.: Condens. Matter. – 2004. – **16**. – P. 9083–9091.
53. *Strong S. T., Pickard C. J, Milman V. et al.* Systematic prediction of crystal structures: an application to sp^3-hybridized carbon polymorphs // Phys. Rev. B. – 2004. – **70**, N 4, art. 045101.
54. *Omata Y., Yamagami Y., Tadano K. et al.* Nanotube nanoscience: a molecular-dynamics study // Physica E. – 2005. – **29**, N 3. – P. 454–468.
55. *Wang J. T., Chen C. F., Kawazoe Y.* Low-temperature phase transformation from graphite to sp^3 orthorhombic carbon // Phys. Rev. Lett. – 2011. – **106**, N 7, art. 075501.
56. *Selli D., Baburin I. A., Martonak R., Leoni S.* Superhard sp^3 carbon allotropes with odd and even ring topologies. – Phys. Rev. B. – 2011. – **84**, N 16, art. 161411 (R).
57. *Amsler M., Flores-Livas J. A., Lehtovaara L. et al.* Crystal structure of cold compressed graphite // Phys. Rev. Lett. – 2012. – **108**, N 6, art. 065501.
58. *Zhao Z. S., Xu B., Zhou X. F. et al*. Novel superhard carbon: c-centered orthorhombic C_8 // Ibid. – 2011. – **107**, N 21, art. 215502.
59. *He C. Y., Sun L. Z., Zhang C. X. et al.* Four superhard carbon allotropes: first-principles study // Phys. Chem. Chem. Phys. – 2012. – **14**, N 23. – P. 8410–8414.
60. *Wang J. T., Chen C. F.* Kawazoe Y. Orthorhombic carbon allotrope of compressed graphite: *ab initio* calculations // Phys. Rev. B. – 2012. – **85**, N 3, art. 033410.
61. *Li D., Bao K., Tian F. B. et al.* Lowest enthalpy polymorph of cold-compressed graphite phase // Phys. Chem. Chem. Phys. – 2012. – **14**, N 13. – P. 4347–4350.
62. *Tian F., Dong X., Zhao Z. S. et al.* Superhard F-carbon predicted by *ab initio* particle-swarm optimization methodology // J. Phys: Condens. Matter. – 2012. – **24**, N 16, art. 165504.
63. N*iu H. Y., Chen X. Q., Wang S. B. et al.* Families of superhard crystalline carbon allotropes constructed via cold compression of graphite and nanotubes // Phys. Rev. Lett. – 2012. – **108**, N 13, art. 135501.
64. *Zhou R. L., Zeng X. C.* Polymorphic phases of sp^3-hybridized carbon under cold compression // J. Am. Chem. Soc. – 2012. – **134**, N 17. – P. 7530–7538.
65. *Amsler M., Flores-Livas J. A., Botti S. et al.* Prediction of a novel monoclinic carbon allotrope, arXiv:1202.6030v1.
66. *Zhu Q., Zeng Q., Oganov A. R.* Systematic search for low-enthalpy sp^3 carbon allotropes using evolutionary metadynamics // Phys. Rev. B. – 2012. – **85**, N 20, art. 201407.
67. *He C. Y., Sun L. Z., Zhang C. X. et al.* New superhard carbon phases between graphite and diamond // Solid. State. Commun. – 2012. – **152**, N 16. – P. 1560–1563.
68. *Zhu Q., Oganov A. R., Salvado M. et al*. Denser than diamond: *ab initio* search for superdense carbon allotropes // Phys. Rev. B. – 2011. – **83**, N 19, art .193410.
69. *Wang Y. C., Lv J., Zhu L., Ma Y. M*. Crystal structure prediction via particle-swarm optimization // Ibid. – 2010. – **82**, N 9, art. 094116.
70. *Wang Y. C., Lv J., Zhu L., Ma Y. M.* CALYPSO: a method for crystal structure prediction // Comp. Phys. Commun. – 2012. – **183**, N 10. – P. 2063–2070.
71. *Goedecker S.* Minima hopping: an efficient search method for the global minimum of the potential energy surface of complex molecular systems // J. Chem. Phys. – 2004. – **120**, N 21. – P. 9911–9917.
72. *Amsler M., Goedecker S*. Crystal structure prediction using the minima hopping method // Ibid. – 2010. – **133**, N 22, art. 224104.
73. *Deaven D. M., Ho K. M.* Molecular geometry optimization with a genetic algorithm // Phys. Rev. Lett. – 1995. – **75**, N 2. – P. 288–291
74. *Niu H. Y., Wei P. Y., Sun Y. et al.* Electronic, optical, and mechanical properties of superhard cold-compressed phases of carbon // Appl. Phys. Lett. – 2011. – **99**, N 3, art. 031901.
75. *Guo X. G., Li L., Liu Z. Y. et al.* Hardness of covalent compounds: roles of metallic component and d valence electrons // J. Appl. Phys. – 2008. – **104**, N 2, art. 023503.
76. *He J. L., Wu E. D., Wang H. T. et al.* Ionicities of boron–boron bonds in B_{12} // Phys. Rev. Lett. – 2005. – **94**, N 1, art. 015504.
77. *Gao F. M., He J. L., Wu E. D. et al.* Hardness of covalent crystals // Ibid. – 2003. – **91**, N 1, art. 015502.
78. *Lyakhov A.O., Oganov A. R.* Evolutionary search for superhard materials: methodology and applications to forms of carbon and TiO_2 // Phys. Rev. B. – 2011. – **84**, N 9, art. 092103.
79. *Zhao Z. S., Xu. B., Wang L. M. et al.* Three dimensional carbon nanotube polymers // ACS. Nano. – 2011. – **5**, N 9. – P. 7726–7234.

80. *Scandolo S., Bernasconi M., Chiarotti G. L. et al.* Pressure-induced transformation path of graphite to diamond // Phys. Rev. Lett. – 1995. – **74**, N 20. – P. 4015–4018.
81. *Zhou X. F., Qian G. R., Dong X. et al.* Ab initio study of the formation of transparent carbon under pressure // Phys. Rev. B. – 2010. – **82**, N 13, art. 13126.
82. *Khaliullin R. Z., Eshet H., Kuhne T. D. et al.* Nucleation mechanism for the direct graphite-to-diamond phase transition // Nat. Mater. – 2011. – **10**, N 1. – P. 693–697.
83. *Boulfelfel S. E., Oganov A. R., Leoni S.* Understanding the nature of "superhard graphite" // Sci. Rep. – 2012. – **2**, art. 471.
84. *Wang Y. J., Panzik J. E. Kiefer B., Lee K. K. M.* Crystal structure of graphite under room-temperature compression and decompression // Ibid. – 2012. – **2**, art. 520.
85. *Paine R. T., Narula C. K.* Synthetic routes to boron nitride // Chem. Rev. – 1990. – **90**, N 1. – P. 73–91.
86. *Hamilton E. J. M., Dolan S. E., Mann C. et al.* Preparation of amorphous boron nitride and its conversion to a turbostratic, tubular form // Science. – 1993. – **260**, N 5108. – P. 659–661.
87. *Chopra N. G., Luyken R. J., Cherrey K. et al*. Boron nitride nanotubes // Ibid. – 1995. – **269**, N 5226. – P. 966–967.
88. *Golberg D., Bando Y., Stephan O., Kurashima K*. Octahedral boron nitride fullerenes formed by electron beam irradiation // Appl. Phys. Lett. – 1998. – **73**, N 17. – P. 2441–2443.
89. *Wentzcovitch R. M., Fahy S., Cohen M. L. Louie S. G*. Ab initio study of graphite → diamond-like transitions in BN // Phys. Rev. B. – 1988. – **38**, N 9. – P. 6191–6193.
90. *Pan Z., Sun H., Zhang Y. Chen C. F.* Harder than diamond: superior indentation strength of wurtzite bn and lonsdaleite // Phys. Rev. Lett. – 2009. – **102**, N 5, art. 055503.
91. *Kern G., Kresse G., Hafner J.* Ab initio calculation of the lattice dynamics and phase diagram of boron nitride // Phys. Rev. B: Condens. Matter. – 1999. – **59**, N 13. – P. 8551–8859.
92. *Johnson Q., Mitchell A. C.* First X-ray diffraction evidence for a phase transition during shock-wave compression // Phys. Rev. Lett. – 1972. – **29**, N 20. – P. 1369–1371.
93. *Meng Y., Mao H. K., Eng P. J. et al.* The formation of sp^3 bonding in compressed BN // Nat. Mater. – 2004. – **3**, N 1. – P. 111–114.
94. *Dong Z., Song Y.* Transformations of cold-compressed multiwalled boron nitride nanotubes probed by infrared spectroscopy // J. Phys. Chem. C. – 2010. – **114**, N 4. – P. 1782–1788.
95. *Yu W. J., Lau W. M., Chan S. P. et al*. *Ab initio* study of phase transformations in boron nitride // Phys. Rev. B. – 2003. – **67**, N 1, art. 014108.
96. *Wang H. B., Li Q., Cui T. et al.* Phase-transition mechanism of hBN → wBN from first principles // Solid. State. Commun. – 009. – **149**, N 21. – P. 843–846.
97. *Wen B., Zhao J. J., Melnik R., Tian Y. J.* Body-centered tetragonal B_2N_2: a novel sp^3 bonding boron nitride polymorph // Phys. Chem. Chem. Phys. – 2011. – **13**, N 32. – P. 14565–14570.
98. *Hromadova L., Martonak R.* Pressure-induced structural transitions in BN from Ab initio metadynamics // Phys. Rev. B. – 2011. – **84**, N 22, art. 224108.
99. *Li Z. P., Gao F. M.* Structure, bonding, vibration, and ideal strength of primitive-centered tetragonal boron nitride // Phys. Chem. Chem. Phys. – 2012. – **14**, N 2. – P. 869–876.
100. *He C. Y., Sun L. Z., Zhang C. X. et al.* Z-BN: a novel superhard boron nitride phase // Phys. Chem. Chem. Phys. – 2012. – **14**, N 31. – P. 10967–10971.
101. *Qi Y., Hector L. G. Jr.* Planar stacking effect on elastic stability of hexagonal boron nitride // Appl. Phys. Lett. – 2007. – **90**, N 8, art. 081922.

Laboratory for Quantum Engineering
and Micro-Nano Energy Technology, Xiangtan University
Hunan Provincial Key Laboratory of Micro-Nano Energy Materials
and Devices, Xiangtan University

Received 21.09.2012